Inorganic Chemistry

Article

pubs.acs.org/IC

Phosphopeptide Selective Coordination Complexes as Promising Src Homology 2 Domain Mimetics

Joel A. Drewry,[†] Eugenia Duodu,[†] Amir Mazouchi,[†] Paul Spagnuolo ,[‡] Steven Burger,[§] Claudiu C. Gradinaru,[†] Paul Ayers,[§] Aaron D. Schimmer,[‡] and Patrick T. Gunning*,[†]

[†]Department of Chemical and Physical Sciences, University of Toronto, 3359 Mississauga Road North, Mississauga, Ontario L5L 1C6, Canada

[‡]Princess Margaret Hospital, Ontario Cancer Institute, 610 University Avenue, Toronto, Ontario M5G 2M9, Canada

[§]Department of Chemistry, McMaster University, 1280 Main Street West, Hamilton, Ontario L8S 4M1, Canada

Supporting Information

ABSTRACT: Src Homology 2 (SH2) domains are the paradigm of phosphotyrosine (pY) protein recognition modules and mediate numerous cancer-promoting protein−protein complexes. Effective SH2 domain mimicry with pY-binding coordination complexes offers a promising route to new and selective disruptors of pY-mediated protein−protein interactions. We herein report the synthesis and in vitro characterization of a library of coordination complex SH2 domain proteomimetics. Compounds were designed to interact with phosphopeptides via a two-point interaction, principally with pY, and to make secondary interactions with pY+2/3, thereby achieving sequence-selective discrimination. Here, we report that lead mimetics demonstrated high target phosphopeptide affinity ($K_a \sim 10^7\ M^{-1}$) and selectivity. In addition, biological screening in various tumor cells for anticancer effects showed a high degree of variability in cytotoxicity among receptors, which supported the proposed two-point binding mode. Several receptors potently disrupted cancer cell viability in breast cancer, prostate cancer, and acute myeloid leukemia cell lines.

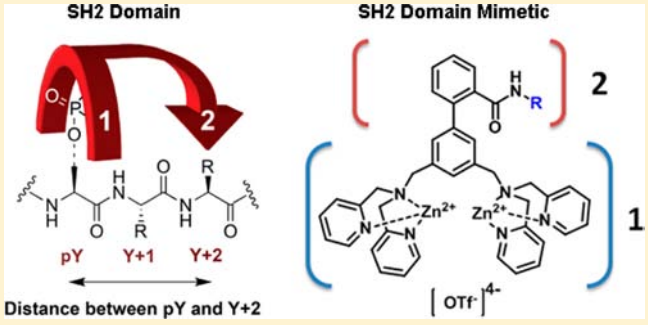

INTRODUCTION

Src Homology 2 (SH2) domains are found ubiquitously in signal transduction proteins such as signal transducers and activator of transcription (STAT), suppressor of cytokine signaling (SOCS), and Src and mediate protein−protein interactions by recognizing specific phosphotyrosine (pY)-containing sequences on a target protein.[1,2] SH2 domains are critical for mediating and regulating cell signaling cascades and have thus become a prominent therapeutic target in cancer research.[3−6] However, small-molecule therapeutics targeting the SH2 domain have, to date, not been successful in the clinic, owing to two major challenges. First, the majority of SH2 domain inhibitors seek to mimic the cognate phosphopeptide binding sequence of a target protein and place a structural emphasis on interacting with the conserved basic amino acids of the SH2 domain's pY binding pocket.[7−9] Consequently, most phosphopeptide mimetics incorporate a polar anionic group, such as a phosphate, to maximize hydrogen-bonding and electrostatic interactions between the inhibitor and the pY binding pocket.[10] Inhibitors of this type have limited cell penetration and suffer from poor pharmacokinetic profiles.[11] Second, while many SH2 domains recognize pY-containing peptide sequences with a high degree of selectivity, others display relative promiscuity for binding partners.[12] It is therefore a significant challenge to identify and exploit structural features of an inhibitor to confer selectivity for a specific SH2 domain, and greater emphasis has been placed in recent years on exploring nontraditional solutions to this problem.[13−15] With this in mind, we recently reported an alternative therapeutic approach, wherein a novel class of ditopic coordination complexes were synthesized to mimic the pY, pY+2 recognition motif employed by SH2 domains to confer phosphoprotein selectivity. The pY recognition element from SH2 domains was mimicked using two proximal zinc(II) dipicolylamine (Zn^{II}DPA) coordination complexes to form dizinc(II) bis(dipicolylamine) (Zn^{II}_2BDPA) subunits, which have been employed extensively in the literature as phosphate monoester recognition units. The pY+X recognition element, which in an SH2 domain is responsible for discriminating between phosphopeptides on the basis of their primary sequence, was mimicked by functionalizing the receptor core in a position computationally predicted to form secondary contacts with a bound peptide (Figure 1). By forming these secondary interactions, receptors were able to form unique

Received: April 23, 2012
Published: July 11, 2012

   dx.doi.org/10.1021/ic3008393 | *Inorg. Chem.* 2012, 51, 8284−8291

contacts with different peptides, resulting in interesting patterns of selectivity.[7]

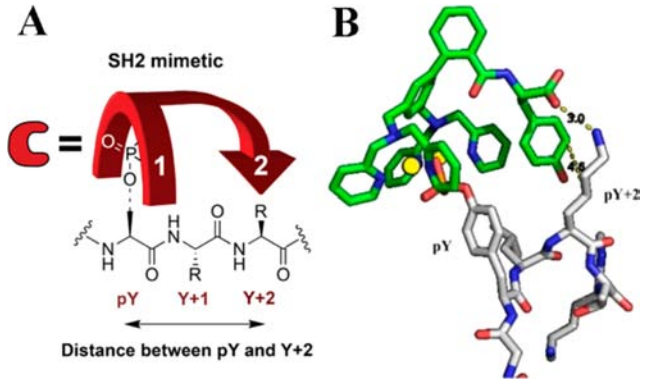

Figure 1. (A) Conceptual illustration of SH2 domain mimicry via the recognition of both pY and adjacent residues. (B) Computationally predicted pY/pY+2/3 binding mode between a previously reported mimetic and a phosphopeptide sequence derived from glycoprotein 130 (GpYLPQTV).

Encouraged by the preliminary data, we herein report the design and synthesis of an extended family of bivalent SH2 domain mimetics (Figure 2) and their in vitro binding affinities and selectivity profiles for a bank of biologically relevant phosphopeptides. The target phosphopeptides selected are found in high-profile cancer targets (Stat1, Stat3, Stat5, Src, IFN-γ, and gp130). We reasoned that selective binding of a target phosphopeptide could facilitate targeted disruption of a phosphopeptide–protein complex in vitro. Thus, receptors were screened for cytotoxicity against cultured breast cancer (MDA 468), prostate cancer (DU 145), and acute myeloid leukemia (AML2) cancer cell lines that contained elevated levels of oncogenic phosphoproteins. In addition, rationalization of in vitro binding data by computational docking analyses of key receptor/phosphopeptide complexes will be presented.

RESULTS AND DISCUSSION

Synthesis of SH2 Domain Mimetics. The synthesis of the expanded library of SH2 domain proteomimetics was achieved as reported previously, with amino acids incorporated into the 2′ position of the biphenyl scaffold (Scheme 1). Briefly, isophthalaldehyde was selectively brominated using *N*-bromosuccinamide in concentrated H_2SO_4. The resultant aryl halide **A** was efficiently coupled to 2-(methoxycarbonyl)phenylboronic acid via microwave-assisted Suzuki coupling protocols to afford biphenyl **7** in high yield. In one pot, using 2 equiv of 2,2′-dipicolylamine and $NaBH(OAc)_3$, dialdehyde **B** was reductively aminated to give **C** in 93% yield.

Next, methyl ester hydrolysis with 2 M NaOH furnished carboxylic acid **D** in excellent yield (90%). Without further purification, **D** was condensed with the desired amino acids using HBTU coupling reagent to afford representative ligand **E**. Coordination complex **15** was prepared by first coupling di-*tert*-butyl-protected tyrosine to **D**, followed by deprotection in 3:1 trifluoroacetic acid/CH_2Cl_2 at room temperature. The treatment of ligands with $Zn^{II}(OTf)_2$ furnished the desired Zn^{II}_2BDPA complexes in excellent yield. The natural diversity of the incorporated amino acid side chains provided a variety of pY+X binding units, ranging from polar-charged groups to large hydrophobic nonpolar groups. A full list of synthesized receptors is shown in Figure 2.

Fluorescence Assays. In previous work,[1,16] it was noted that lifetime suppression took place when fluorescently labeled phosphopeptides (herein denoted F*-peptide) were bound by Cu^{II}_2BDPA metal complexes. We therefore reasoned that it was possible that the synthesized family of Zn^{II}_2BDPA metal

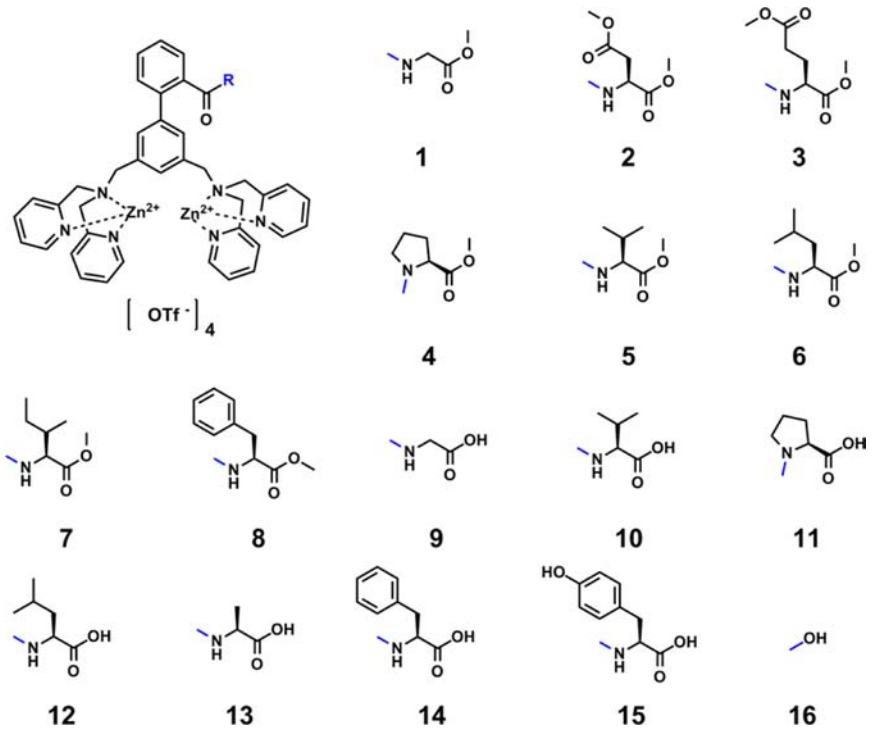

Figure 2. Synthesized library coordination-complex-based SH2 domain mimetics.

dx.doi.org/10.1021/ic3008393 | *Inorg. Chem.* 2012, 51, 8284–8291

Scheme 1. Synthesis of Phosphopeptide-Selective Receptors

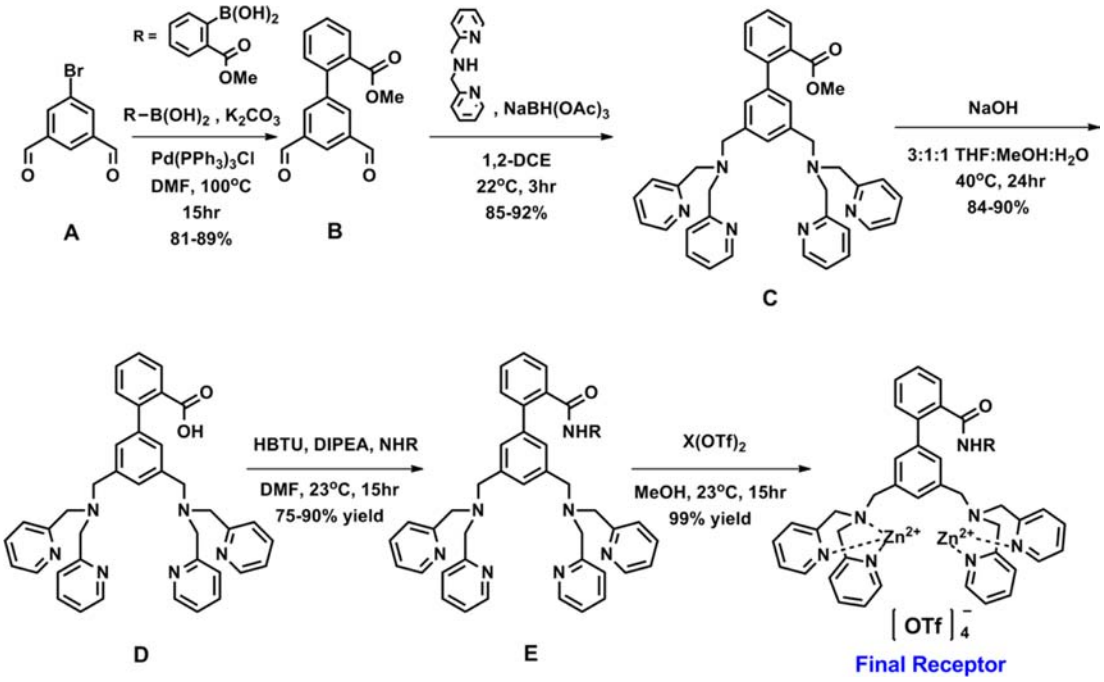

complexes (mimetic library) could exhibit the same effect. Accordingly, we sought to investigate the fluorescence character of the mimetic/phosphopeptide interaction using a randomly selected receptor, **11**, a fluorescein-labeled phosphopeptide derived from the erythropoietin (EPO) receptor (5-FAM-GpYLVLDKW-NH_2), and its natural high-affinity binding partner Stat5 protein.[17]

Excitedly, coincubation of the labeled peptide (20 nM) and **11** (100 μM) resulted in a 96% reduction in the fluorescence intensity, indicating a strong quenching of the dye. Interestingly, the fluorescence lifetime of the dye (3.76 ns) increased by ~15% (4.35 ns), which seems contradictory with the strong quenching observed. In addition, fluorescence lifetime analysis revealed that monoexponential decay of fluorescence occurred in both the presence and absence of **11** (100 μM; Figure 3). This finding was consistent with a single population of fluorescent species (i.e., quenched or unquenched) and indicated that either collisional or static quenching was taking place but not both.

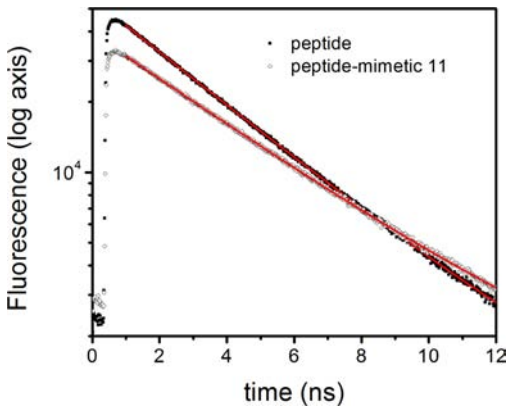

Figure 3. Fluorescence lifetime histogram showing enhanced monoexponential decay in the presence of **11**.

The addition of 300 nM Stat5, a natural and strong binding partner of the labeled peptide, to the solution of peptide and mimetic **11** recovered the fluorescence intensity to 23% of the intensity observed for the labeled peptide alone. This suggested that the peptide bound by Stat5 is either not quenched or significantly less quenched by the mimetic and is consistent with a scenario wherein mimetic-bound peptide is statically quenched and free or protein-bound peptide is unquenched.

To probe our hypothesis that the reduction in the fluorescence intensity of the bound peptide was the result of static quenching, fluorescence correlation spectroscopy (FCS) was used to evaluate the relative proportion of fluorescently active species in the system (Table 1). Diffusion correlation

Table 1. FCS Analysis of the Fluorescent Species in Samples Involving 11 and a Model Fluorescein-Labeled EPO[a]

τ_d (μs)	73±3	345±18	83±4
Samples	Fractions (%)		
+	3		96
+	79	21	
+ +	19	4	77
peptide Stat5 mimetic 11			
peptide-Stat5 peptide-mimetic 11			

[a]The peptide/mimetic **11** complex was not fluorescent because of static quenching, and its fraction was determined based on the reduction of the overall fluorescence intensity.

times were recorded for labeled peptide alone, as well as in the presence of Stat5 and/or mimetic **11**. Labeled peptide alone was determined to have a small correlation time of 73 μs, whereas Stat5-bound labeled peptide had a predictably larger correlation time of 345 μs. Interestingly, it was possible to acquire correlation data from a sample exhibiting very strong quenching (20 nM F*-peptide and 100 μM mimetic **11**) in a

dx.doi.org/10.1021/ic3008393 | Inorg. Chem. 2012, 51, 8284–8291

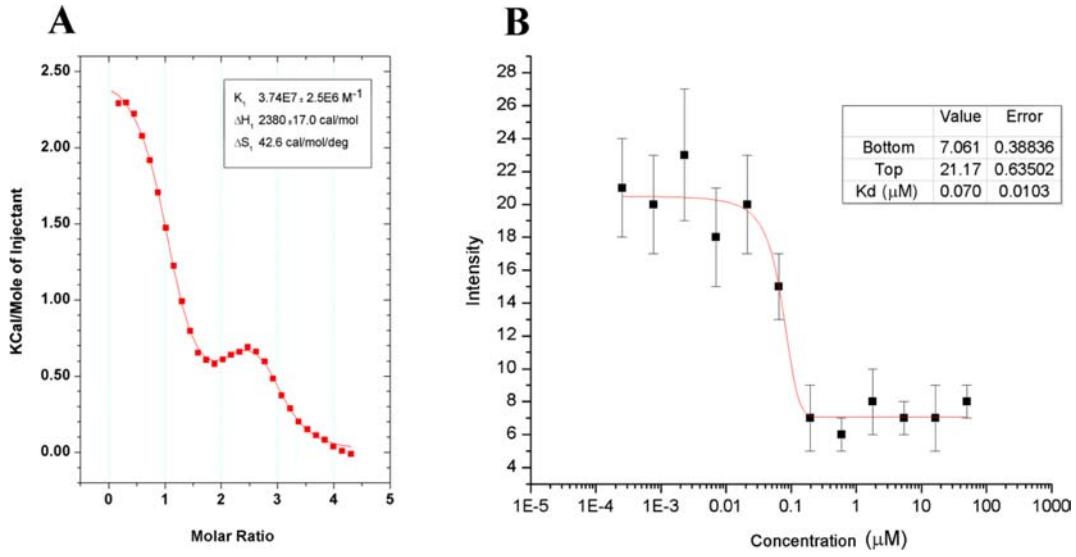

Figure 4. (A) ITC trace showing high-affinity stoichiometric binding between **11** and EPO (K_a = 3.74 ± 0.25 × 10^7 M^{-1}). (B) Titration in which labeled EPO (10 nM) was coincubated with **11** (2 nM to 100 μM), depicting the dose-dependent decrease in the fluorescence intensity (K_a = 1.7 ± 0.7 × 10^7 M^{-1}).

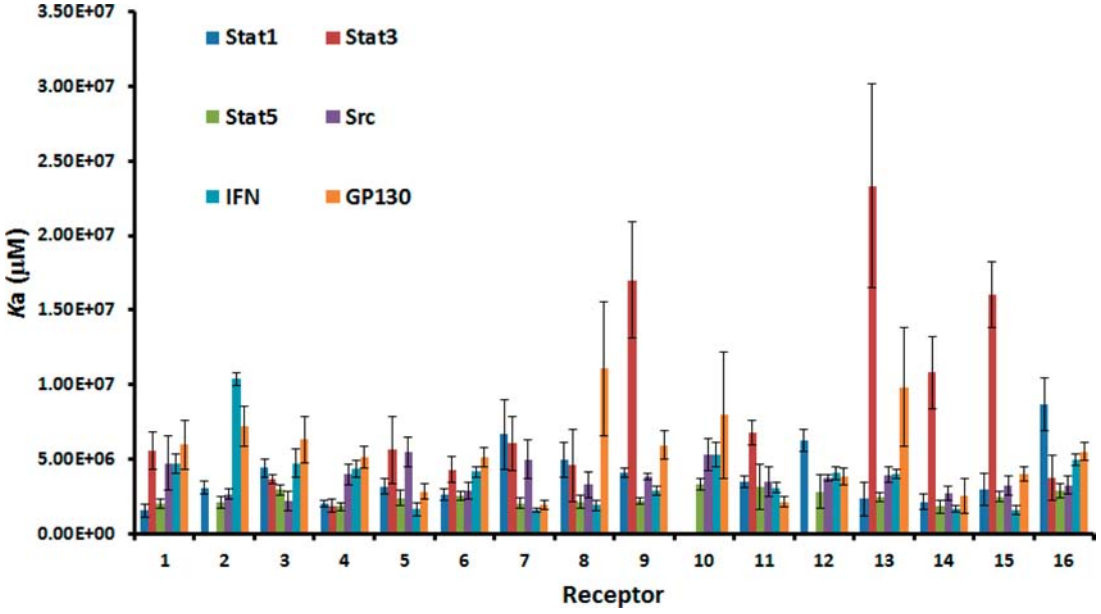

Figure 5. K_a values generated through the fluorescence intensity assay (10 nM peptide, pH 7.3, 25 °C.

microscope setup as described previously.[18] The low concentration of fluorescence species estimated by our analysis (~0.9 nM) indicates the presence of a small nonquenched peptide fraction (<5%) in solution with a slightly increased correlation time (83 μs). While adding Stat5 to this system predictably resulted in the generation of a population of Stat5-bound peptide, the relative proportions of Stat5-bound to free peptide were essentially identical with those in the system that did not contain **11**.

Taken together, the fluorescence intensity, lifetime, and FCS data proved that complexation between the mimetic and the labeled peptide resulted in static quenching of the peptide's fluorescence. Such an effective quenching leads to a two-state system involving the peptide and mimetic: when bound by a mimetic, the peptide was strongly quenched, while the unbound peptide was bright. Subsequent titrations, where the fluorescence intensity of a labeled phosphopeptide was plotted as a function of the mimetic concentration, were compared to the results of isothermal titration calorimetry (ITC) measurements of mimetic/phosphopeptide binding affinities, which showed conclusively that the fluorescence intensity was a reliable and accurate marker for peptide/mimetic binding (Figure 4)

Receptor/Phosphopeptide Affinity Constants. To measure binding affinities between the mimetic library and the bank of biologically relevant peptides, the protocol for the fluorescence intensity assay was adopted for high-throughput screening using a 374-well plate reader/fluorimeter. Consistent with previous findings, modulation at the 2′ position of the biphenyl scaffold afforded a library with a wide variance in selectivity (Figure 5).

dx.doi.org/10.1021/ic3008393 | Inorg. Chem. 2012, 51, 8284−8291

Interestingly, several of the hydrolyzed ester derivatives bearing a carboxylic acid group (**9**, **11**, and **13**−**15**) displayed pronounced selectivity for the phosphopeptide derived from the oncogenic transcription factor signal transducer and activator of transcription (Stat3; 5-FAM-GpYLKTK-NH_2). This finding validated our previous hypothesis that Stat3 sequence selectivity was derived from interaction between the terminal anionic carboxylate of the receptor and the cationic lysine residue of Stat3, located at the pY+2 position. Because Stat3 is considered to be a master regulator of cancer development and apoptotic resistance, this result was especially encouraging. Mimetics featuring neutral pendants (**1**−**8**) displayed unique binding preferences, although, notably, selectivity was not observed for any of the six peptides tested. As a control, compound **16** was prepared, lacking a binding group at the 2′ position of the upper phenyl ring. As expected, compound **16**, not equipped with a pendant group and thus unable to form significant secondary binding contacts, was found to have negligible phosphopeptide selectivity comparable to the least selective of the derivatized mimetics. Thus, appropriate functionalization of the 2′ position of the biphenyl-based scaffold imparts an otherwise nonselective phosphopeptide receptor, with functionality critical to SH2 domain mimicry. Our binding data demonstrate that artificial SH2 domain mimetics can discriminate similar phosphopeptides on the basis of their pY+X sequence identity.

Receptor Cytotoxicity Screening against Cancer Cells (MDA468, DU145, and AML2 Lines). Given the diversity of the phosphopeptide selectivity observed, we reasoned that select compounds might disrupt key phosphorylation-mediated protein−protein interactions in whole cancer cells and therefore function as potential chemotherapeutic agents. Thus, compounds were screened for cytotoxicity using a standard CellTiter96 aqueous nonradioactive (MTS) assay. Briefly, cancer cell lines were coincubated with compounds **1**−**16** or dimethyl sulfoxide at 37 °C for 3 days, after which time the percentage of remaining viable cells was quantified by treatment with MTS, which is metabolized into a fluorescent indicator by healthy, viable mitochondria.

Excitedly, several compounds were highly cytotoxic against cells derived from breast cancer (MDA468), prostate cancer (DU145), and especially acute myeloid leukemia (AML2) (Table 2). Compound **8**, previously reported as a selective binder to the phosphopeptide derived from the gp130 receptor, demonstrated remarkably potent anticancer activity, with IC_{50} values against MDA468, DU145, and AML2 of 5.0 ± 1.0, 16.8 ± 2.5, and 1.3 ± 0.8 μM, respectively. Interestingly, while highly selective for the Stat3 sequence in the fluorescence intensity assay, compounds **13** and **14** were not active against any of the tested cell lines, including MDA468, which is known to critically depend on the Stat3 function. On the other hand, compound **15**, previously reported as a Stat3-selective SH2 domain mimetic in fluorescence experiments, was highly active against both MDA468 and DU145. Inconsistencies between the fluorescence intensity and cytotoxicity data are most likely the result of a receptor possessing higher binding affinity with another untested phosphopeptide/protein inside the cell or poor cell permeability.

The variable cytotoxicity exhibited by this family of receptors might be a result of phosphopeptide/protein selectivity being displayed in vitro. If all compounds showed similar activity against the tested cancer cell lines, it would stand to reason that each compound was targeting the same phosphorylated targets and, in turn, that functionalization at the 2′ position had no directing effect on the receptor's selectivity. Instead, we observed a spectrum of activity in the different cell lines. Moreover, compound **16**, which is not equipped with an amino acid and is therefore minimally equipped to interact with regions adjacent to a phosphorylated residue, was observed to be the least biologically active receptor tested, with IC_{50} values exceeding 100 μM in each cell line. This suggests that the therapeutic potential of these compounds is derived through a more targeted biological effect and not simply through general toxicity.

Table 2. MTS Cytotoxicity Screen of SH2 Domain Proteomimetics versus Common Cancer Cell Lines

	MDA468		DU145		AML2	
	IC_{50} (μM)	±	IC_{50} (μM)	±	IC_{50} (μM)	±
1	>50		>50		>50	
2	>50		>50		8.8	1.4
3	8.1	0.4	>50		5.3	4.1
4	>50		>50		>50	
5	6.2	1.3	29.8	3.4	12.2	0.4
6	>50		>50		5.8	1.2
7	>50		25.2	4.6	25.2	1.0
8	5.0	1.0	16.8	2.5	1.3	0.8
9	>50		>50		>50	
10	>50		>50		>50	
11	16.0	0.7	38.2	3.3	34.3	5.0
12	>50		>50		>50	
13	>50		>50		>50	
14	>50		>50		>50	
15	24.7	2.6	19.3	3.6	>50	
16	>50		>50		>50	

CONCLUSIONS

We have reported the synthesis of a small library of ditopic phosphopeptide receptors equipped with both pY and pY+2 binding motifs. Using a fluorescence intensity assay, we demonstrated that, consistent with our hypothesis, placing functionality at the 2′ position confers to the receptor the ability to interact with region(s) adjacent to the pY. Furthermore, this, in turn, affords the mimetic the capacity to discriminate between similar peptides on the basis of their primary sequence. Further supporting this result was the finding that the reported family of mimetics displayed a wide variance in cytotoxicity against common cancer cell lines. While we cannot predict that the phosphopeptide selectivity observed in the fluorescence intensity screen reflects target selectivity inside the cell, we have demonstrated that specific pY+2 functionality does confer varying biological activity. This is best observed when **16**, containing no pY+2 binders and being nontoxic, is compared to **8**, containing a phenylalanine functional group, which shows most potent activity against AML2 cancer cells (IC_{50} ∼ 1 μM). Biochemical and biological studies are now ongoing to determine the intracellular effects of these lead compounds, the results of which will be published elsewhere. In summary, this proof-of-principle study suggests that simple, dinuclear zinc(II) complexes can be rationally and computationally engineered into functional mimetics of SH2 domains, a prominent class of protein subdomains critical to cell signaling.

dx.doi.org/10.1021/ic3008393 | Inorg. Chem. 2012, 51, 8284−8291

EXPERIMENTAL SECTION

General Procedures. Anhydrous solvents methanol (MeOH), dimethyl sulfoxide (DMSO), CH_2Cl_2, tetrahydrofuran (THF), and *N*,*N*-dimethylformamide (DMF) were purchased from Sigma Aldrich and used directly from Sure-Seal bottles. Molecular sieves were activated by heating to 300 °C under vacuum overnight. All reactions were performed under atmospheric conditions in oven-dried glassware and were monitored for completeness by thin-layer chromatography (TLC) using silica gel (visualized by UV light or developed by treatment with $KMnO_4$ or phosphomolybdic acid stain). All reactions, with the exception of the metal complexations, were carried out in a Biotage Initiator microwave at temperatures and durations indicated in the representative synthesis shown in the Supporting Information. ^{1}H and ^{13}C NMR spectra were recorded on Bruker 400 MHz and Varian 500 MHz spectrometers in either $CDCl_3$, CD_3OD, or DMSO-d_6. Chemical shifts (δ) are reported in parts per million after calibration to a residual isotopic solvent. Coupling constants (J) are reported in hertz. Purification of scaffolds prior to metal coordination was achieved using flash chromatography (silica). The ligand purity was confirmed by analytical rpHPLC using linear gradients from 100% 0.01 M NH_4OAc(aq) (A) to 100% MeOH (B), with changing solvent composition of either (I) 6.25%/min or (II) 9.34%/min after an initial 2 min of 100% A.

Fluorescence Assay. Screens were conducted using Corning Black 384 well plates in a Tecan M1000 fluorimeter with a plate reader. Each well contained 10 nM phosphopeptide in 50 mM *N*-(2-hydroxyethyl)piperazine-*N*′-2-ethanesulfonic acid buffer (pH 7.3, 25 °C) and a variable concentration of the receptor (~1 nM to ~200 μM). *Z* depth and gain were both cell-optimized by the system automatically. Concentrations exceeding 100 μM were not used in order to avoid fluorescence quenching due to collisional nonbinding events. Each receptor was screened in triplicate on two separate occasions, with data averaged to ensure accurate K_d values. Binding constants were obtained using nonlinear logistic fitting in *Origin 8*.

Cytotoxicity Screen. Human OCI-AML2 leukemia, DU145 prostate cancer, and MDA468 breast cancer cells were seeded in 96-well plates. Cells were then treated with increasing concentrations of receptors **1**−**16**. A total of 70 h after incubation, the cell growth and viability was measured with the MTS assay according to the manufacturer's instructions (Promega, Madison, WI) and as described previously.[19] Data represent the mean IC_{50} + SD (n = 3).

Coupling of the Ligand Precursor D to L-Amino Acids. To a stirring solution of **D** (1.0 equiv) in DMF (0.1 M) was added HBTU (1.2 equiv) in one portion. Following 10 min of stirring, amino acid (1.1 equiv) and DIPEA (2.5−3.5 equiv) were added sequentially. The solution was then heated (microwave-assisted) to 65 °C and allowed to react for 25 min. When TLC indicated completion, the solution was poured into saturated, aqueous sodium bicarbonate and extracted several times into ethyl acetate. The organic fractions were then combined and washed four times with a saturated sodium bicarbonate solution, dried over sodium sulfate, and concentrated in vacuo.

Hydrolysis of Ligand Precursors E (Compounds 9−15). To a stirring solution of methyl-esterified ligand precursor **E** (1.0 equiv) in 3:1:1 THF/MeOH/H_2O (0.1 M) was added LiOH·H_2O (2.0 equiv) in one portion. The mixture was stirred for approximately 5 min to ensure that the base had evenly dissolved, after which it was heated (microwave assisted) to 65 °C and allowed to react for 14 min. When TLC indicated completion, the solution was neutralized using 4 M HCl/dioxane and concentrated in vacuo.

Zinc(II) Metal Coordination to Ligands 1−16. Following purification by silica gel chromatography, the final scaffolds were dissolved in anhydrous MeOH, zinc(II) triflate (2.0 equiv) was added in one portion, and the solution was allowed to stir overnight at room temperature. MeOH was then removed in vacuo, and the resulting solid was washed twice with ether to remove unreacted scaffold. The solid was then redissolved in a small volume of MeOH and filtered through National Scientific Target Syringe Filters (Cellulose Acetate Membrane; 4 mm, 0.20 μm). Finally, the filtrate was diluted in distilled water and lyophilized to dryness.

Characterization of Final Ligand Precursors E (L1−L16) and Final Complexes 1−16. L1. ^{1}H NMR (400 MHz, $CDCl_3$): δ_H 3.42 (s, 3H, $-OCH_3$), 3.65 (d, J = 5.0 Hz, 2H, $C_\alpha H_2$), 3.70 (s, 4H, $PhCH_2N-$), 3.79 (s, 8H, $-NCH_2Pyr$), 6.04 (s, 1H, NH), 7.10 (t, J = 6.0 Hz, 4H, CH (Ar)), 7.27 (d, J = 6.0 Hz, 1H, CH (Ar)), 7.32 (s, 2H, CH (Ar)), 7.37−7.52 (m, 3H, CH (Ar)), 7.54−7.65 (m, 8H, CH (Ar)), 7.73 (d, J = 8.0 Hz, 1H, CH (Ar)), 8.46 (d, J = 4.2 Hz, 4H, CH (Ar)). ^{13}C NMR (400 MHz, $CDCl_3$): δ_C 41.2, 51.8, 58.4, 59.9, 121.8, 122.7, 127.4, 128.9, 130.2, 130.3, 134.5, 136.3, 139.5, 139.8, 140.1, 148.8, 159.5, 161.1, 161.4. HRMS (ES^+). Calcd for $C_{42}H_{42}N_7O_3$ [M + H]: m/z 692.3344. Found: m/z 692.3350. IR (KBr, cm^{-1}): 3449, 3004, 2923, 2804, 1753, 1664, 1592, 1570, 1541, 1470, 1431, 1357, 1208, 1170, 1046, 759.

1. HRMS (ES^+). Calcd for $C_{42}H_{41}N_7O_3Zn_2$ [M]: m/z 819.1832. Found: m/z 819.1845. IR (KBr, cm^{-1}): 3449, 2917, 1635, 1539, 1445, 264, 1229, 1177, 1034, 765.

L2. ^{1}H NMR (400 MHz, $CDCl_3$): δ_H 2.92 (dd, J = 17.3 and 4.6 Hz, 1H, $C_\beta H$), 2.61 (dd, J = 17.3 and 4.6 Hz, 1H, $C_\beta H$), 3.31 (s, 3H, CO_2CH_3), 3.42 (s, 3H, CO_2CH_3), 3.63−3.87 (m, 12H, $PhCH_2N-$ and $-NCH_2Pyr$), 4.61−4.67 (m, 1H, $C_\alpha H$), 6.35 (d, J = 8.2 Hz, 1H, NH), 7.08−7.13 (t, J = 6.1 Hz, 4H, CH (Ar)), 7.28−7.34 (m, 3H, CH (Ar)), 7.40 (t, J = 7.3 Hz, 1H, CH (Ar)), 7,47 (t, J = 7.3 Hz, 7.50 (s, 1H, CH (Ar)), 7.55−7.70 (m, 9H, CH (Ar)), 8.48 (d, J = 4.9 Hz, 4H, CH (Ar)). ^{13}C NMR (400 Hz, $CDCl_3$): δ_C 35.3, 48.0, 51.4, 52.4, 58.3, 60.0, 76.6, 77.0, 77.2, 121.8, 122.7, 127.4, 127.7, 128.2, 128.6, 130.2, 130.4, 134.8, 136.4, 139.5, 139.6, 140.0, 148.8, 159.5, 168.9, 170.4, 170.6. HRMS (ES^+). Calcd for $C_{45}H_{46}N_7O_5$ [M + H]: m/z 764.3555. Found: m/z 764.3571. IR (KBr, cm^{-1}): 3440, 2922, 2851, 1736, 1648, 1593, 1474, 1434, 1366, 1216, 1154, 763.

2. HRMS (ES^+). Calcd for $C_{45}H_{45}N_7O_5Zn_2$ [M]: m/z 891.2043. Found: m/z 891.2063. IR (KBr, cm^{-1}): 3483, 2923, 1736, 1637, 1609, 1574, 1444, 1259, 1230, 1174, 1100, 1034, 766.

L3. ^{1}H NMR (400 MHz, $CDCl_3$): δ_H 1.49−1.96 (m, 4H, $C_\beta H_2C_\gamma H_2$), 3.35 (s, 3H, CO_2CH_3), 3.46 (s, 3H, CO_2CH_3), 3.72 (s, 4H, $PhCH_2N-$), 3.83 (s, 8H, $-NCH_2Pyr$), 4.31−4.38 (m, 1H, $C_\alpha H$), 6.03 (d, J = 8.1 Hz), 7.08−7.16 (m, 4H, CH (Ar)), 7.27−7.71 (m, 15H, CH (Ar)), 8.48 (s, 4H, CH (Ar)). ^{13}C NMR (400 Hz, $CDCl_3$): δ_C 26.9, 29.2, 51.4, 52.0, 58.2, 59.8, 76.6, 76.9, 77.2, 121.9, 122.7, 127.4, 127.9, 128.6, 130.1, 130.3, 134.9, 136.4, 139.6, 140.2, 148.8, 159.3, 169.1, 171.3, 172.4. HRMS (ES^+). Calcd for $C_{46}H_{48}N_7O_5$ [M + H]: m/z 778.3711. Found: m/z 778.3712. IR (KBr, cm^{-1}): 3438, 2922, 2847, 1736, 1645, 1593, 1569, 1536, 1474, 1434, 1366, 1209, 1170, 1047, 995, 763.

3. HRMS (ES^+). Calcd for $C_{46}H_{47}N_7O_5Zn_2$ [M]: m/z 905.2200. Found: m/z 905.2203. IR (KBr, cm^{-1}): 3473, 1732, 1643, 1609, 1574, 1530, 1484, 1445, 1263, 1229, 1175, 1033, 765.

L4. ^{1}H NMR (400 MHz, $CDCl_3$): δ_H 0.92−1.6 (m, 4H, ring CH_2), 2.61−3.11 (m, 1H, ring CH_2), 3.34−3.85 (m, 15H, $PhCH_2N-$ and $-NCH_2Pyr$ and $-OCH_3$), 4.15 (s, 1H, $C_\alpha H$), 7.05−7.13 (s, 4H, CH (Ar)), 7.30−7.51 (m, 7H, CH (Ar)), 7.55−7.67 (m, 8H, CH (Ar)), 8.46 (d, J = 4.8 Hz, 4H, CH (Ar)). ^{13}C NMR (400 Hz, $CDCl_3$): δ_C 22.4, 24.0, 29.0, 30.3, 47.7, 51.8, 58.1, 58.3, 58.4, 59.8, 76.6, 77.0, 77.2, 77.3, 121.8, 122.6, 122.7, 127.4, 127.5, 127.7, 127.9, 128.8, 129.4, 129.5, 135.9, 136.5, 139.3, 139.6, 139.8, 148.8, 159.3, 159.4, 169.7, 172.0. HRMS (ES^+). Calcd for $C_{45}H_{46}N_7O_3$ [M + H]: m/z 732.3657. Found: m/z 732.3651. IR (KBr, cm^{-1}): 3432, 2923, 1742, 1629, 1593, 1568, 1434, 1199, 1174, 1091, 996, 763.

4. HRMS (ES^+). Calcd for $C_{45}H_{45}N_7O_3Zn_2$ [M]: m/z 859.2145. Found: m/z 859.2160. IR (KBr, cm^{-1}): 3443, 1736, 1630, 1483, 1445, 1262, 1229, 1177, 1034, 765.

L5. ^{1}H NMR (400 MHz, $CDCl_3$): δ_H 0.37 (dd, J = 17.0 and 6.9 Hz, 6H, $-CH(CH_3)_2$), 1.61−1.74 (m, 1H, $-CH(CH_3)_2$), 3.40 (s, 3H, CO_2CH_3), 3.69 (s, 4H, $PhCH_2N-$), 3.79 (s, 8H, $-NCH_2Pyr$), 4.26 (dd, J = 8.3 and 4.8 Hz, 1H, $C_\alpha H$), 5.81 (d, J = 8.3 Hz, 1H, NH), 7.07−7.13 (m, 4H, CH (Ar)), 7.27 (dd, J = 7.5 and 1.3 Hz, 1H, CH (Ar)), 7.38−7.48 (m, 4H, CH (Ar)), 7.51−7.70 (m, 10H, CH (Ar)), 8.47 (d, J = 5.1 Hz, 4H, CH (Ar)). ^{13}C NMR (400 Hz, $CDCl_3$): δ_C 17.3, 18.2, 30.8, 51.7, 57.2, 58.3, 59.9, 76.6, 76.9, 77.2, 121.8, 122.6, 127.4, 127.7, 128.3, 128.7, 130.0, 130.4, 135.1, 136.4, 139.5, 139.7, 140.3, 148.8, 159.4, 169.1, 171.4. HRMS (ES^+). Calcd for $C_{45}H_{48}N_7O_3$

dx.doi.org/10.1021/ic3008393 | *Inorg. Chem.* 2012, 51, 8284−8291

[M + H]: m/z 734.3813. Found: m/z 734.3816. IR (KBr, cm^{-1}): 3441, 3059, 2962, 2820, 1740, 1649, 1593, 1569, 1534, 1474, 1434, 1365, 1207, 1155, 1047, 764.

5. HRMS (ES^+). Calcd for $C_{45}H_{47}N_7O_3Zn_2$ [M]: m/z 861.2301. Found: m/z 861.2310. IR (KBr, cm^{-1}): 3450, 2916, 2848, 2358, 1740, 1637, 1575, 1539, 1263, 1229, 1176, 1033, 765.

L6. ^1H NMR (400 MHz, $CDCl_3$): δ_H 0.50 (t, J = 5.7 Hz, 6H, $-CH(CH_3)_2$), 0.94−1.05 (m, 2H, $-C_\beta H_2$), 1.09−1.21 (m, 1H, $-CH(CH_3)_2$), 3.40 (s, 3H, CO_2CH_3), 3.69 (s, 4H, $PhCH_2N-$), 3.78 (s, 8H, $-NCH_2Pyr$), 4.26−4.34 (m, 1H, $C_\alpha H$), 5.74 (d, J = 8.2 Hz, 1H, NH), 7.05−7.12 (m, 4H, CH (Ar)), 7.26 (d, J = 7.6 Hz, 1H, CH (Ar)), 7.34−7.46 (m, 2H, CH (Ar)), 7.52−7.70 (m, 10H, CH (Ar)), 8.46 (d, J = 4.8 Hz, 4H, CH (Ar)). ^{13}C NMR (400 Hz, $CDCl_3$): δ_C 21.7, 22.2, 24.2, 41.1, 50.7, 51.8, 58.2, 59.9, 76.6, 77.7, 77.2, 77.3, 121.8, 122.7, 127.4, 127.8, 128.2, 128.7, 130.0, 130.3, 135.0, 136.4, 139.5, 139.6, 140.3, 148.8, 159.4, 168.9, 172.5. HRMS (ES^+). Calcd for $C_{46}H_{50}N_7O_3$ [M + H]: m/z 748.3970. Found: m/z 748.3982. IR (KBr, cm^{-1}): 3422, 3056, 2953, 2362, 1742, 1650, 1592, 1569, 1473, 1433, 1367, 1204, 1161, 1047, 995, 762.

6. HRMS (ES^+). Calcd for $C_{46}H_{49}N_7O_3Zn_2$ [M]: m/z 875.2458. Found: m/z 875.2452. IR (KBr, cm^{-1}): 3473, 2957, 1741, 1636, 1610, 1445, 1262, 1230, 1174, 1034, 765.

L7. ^1H NMR (400 MHz, $CDCl_3$): δ_H 0.33 (d, J = 7.1 Hz, 3H, $-CH_3$), 0.49 (t, J = 7.1 Hz, 3H, $-CH_3$), 0.52−0.98 (m, 2H, $C_\gamma H_2$), 1.35−1.46 (m, 1H, $C_\beta H$), 3.41 (s, 3H, CO_2CH_3), 3.69 (s, 4H, $PhCH_2N-$), 3.80 (s, 8H, $-NCH_2Pyr$), 4.32 (q, J = 8.3 and 4.6 Hz, 1H, $C_\alpha H$), 5.83 (d, J = 8.3 Hz, 1H, NH), 7.10 (t, J = 5.8 Hz, 4H, CH (Ar)), 7.28 (d, J = 7.7 Hz, 1H, CH (Ar)), 7.33−7.48 (m, 4H, CH (Ar)), 7.50−7.71 (m, 10H, CH (Ar)), 8.48 (d, J = 5.0 Hz, 4H, CH (Ar)). ^{13}C NMR (400 Hz, $CDCl_3$): δ_C 11.2, 14.0, 14.6, 24.7, 37.5, 51.6, 56.5, 58.3, 59.9, 60.2, 76.6, 76.9, 77.1, 77.2, 121.8, 122.7, 127.4, 127.7, 128.2, 128.7, 130.0, 130.4, 135.1, 136.4, 139.5, 139.7, 140.3, 148.7, 159.4, 168.9, 171.4. HRMS (ES^+). Calcd for $C_{46}H_{50}N_7O_3$ [M + H]. IR (KBr, cm^{-1}): 3439, 2961, 2922, 1739, 1647, 1592, 1569, 1473, 1433, 1364, 1202, 1150, 762.

7. HRMS (ES^+). Calcd for $C_{46}H_{49}N_7O_3Zn_2$ [M]: m/z 875.2458. Found: m/z 875.2444. IR (KBr, cm^{-1}): 3449, 1638, 1446, 1262, 1175, 1034, 765.

L8. ^1H NMR (400 MHz, $CDCl_3$): δ_H 2.54−2.78 (m, 2H, $-CH_2Ph$), 3.31 (s, 3H, CO_2CH_3), 3.63−3.90 (m, 12H, $PhCH_2N-$ and $-NCH_2Pyr$), 4.51−4.63 (m, 1H, $C_\alpha H$), 5.87 (d, J = 7.5 Hz, 1H, NH), 6.63 (d, J = 7.8 Hz, 2H, CH (Ar)), 6.96−7.14 (m, 8H, CH (Ar)), 7.26−7.48 (m, 6H, CH (Ar)), 7.51−7.66 (m, 11H, CH (Ar)), 8.47 (d, J = 4.86 Hz, 4H, CH (Ar)). ^{13}C NMR (400 Hz, $CDCl_3$): δ_C 37.8, 52.0, 53.4, 58.5, 60.1, 76.8, 77.2, 77.4, 77.5, 122.1, 122.9, 126.9, 127.6, 128.1, 128.4, 128.6, 128.7, 129.0, 130.3, 130.6, 135.1, 135.5, 136.6, 139.7, 140.3, 149.0, 159.6, 169.1, 171.2. HRMS (ES^+). Calcd for $C_{49}H_{48}N_7O_3$ [M + H]: m/z 732.3813. Found: m/z 732.3824. IR (KBr, cm^{-1}): 3426, 3060, 2922, 2819, 1742, 1643, 1592, 1432, 1362, 1214, 1150, 994, 761.

8. HRMS (ES^+). Calcd for $C_{49}H_{47}N_7O_3Zn_2$ [M]: m/z 909.2301. Found: m/z 909.2312. IR (KBr, cm^{-1}): 3476, 1742, 1610, 1574, 1445, 1252, 1171, 1100, 1034, 766.

L9. ^1H NMR (400 MHz, $CDCl_3$): δ_H 3.76 (s, 4H, $PhCH_2N-$), 3.84 (d, J = 5.8 Hz, 2H, $C_\alpha H_2$), 3.90 (s, 8H, $-NCH_2Pyr$), 6.28 (s, 1H, NH), 7.15 (t, J = 6.0, 4H, CH (Ar)), 7.28 (s, 1H, CH (Ar)), 7.33−7.49 (m, 6H, CH (Ar)), 7.54 (d, J = 7.7, 4H, CH (Ar)), 7.65 (t, J = 7.4 and 2.0 Hz, 4H, CH (Ar)), 7.78 (dd, J = 7.3 and 1.7 Hz, 1H, CH (Ar)), 8.49 (d, J = 4.3 Hz, 4H, CH (Ar)). ^{13}C NMR (400 MHz, $CDCl_3$): δ_C 42.7, 58.4, 59.0, 122.3, 123.6, 127.5, 128.7, 128.9, 129.9, 130.0, 130.4, 135.0, 137.1, 138.3, 139.7, 140.7, 148.3, 157.9, 168.8, 171.3. HRMS (ES^+). Calcd for $C_{41}H_{40}N_7O_3$ [M + H]: m/z 678.3187. Found: m/z 678.3156. IR (KBr, cm^{-1}): 3414, 2923, 2851, 1647, 1594, 1570, 1534, 1474, 1436, 1384, 1299, 1151, 998, 765.

9. HRMS (ES^+). Calcd for $C_{41}H_{39}N_7O_3Zn_2$ [M]: m/z 805.1675. Found: m/z 805.1670. IR (KBr, cm^{-1}): 3480, 2924, 2855, 1735, 1627, 1609, 1445, 1275, 1255, 1171, 1033, 839, 766.

L10. ^1H NMR (400 MHz, $CDCl_3$): δ_H 0.79 (dd, J = 26.8 and 6.9 Hz, 6H, $-CH(CH_3)_2$), 1.95−2.11 (m, 1H, $-CH(CH_3)_2$), 3.64−3.92 (m, 12H, $PhCH_2N-$ and $-NCH_2Pyr$), 4.34 (dd, J = 8.40 and 4.9 Hz, 1H, $C_\alpha H$), 6.13 (d, J = 8.3 Hz, 1H, NH), 7.13 (t, J = 6.3 Hz, 4H, CH (Ar)), 7.29 (d, J = 7.7 Hz, 1H, CH (Ar)), 7.37−7.58 (m, 9H, CH (Ar)), 7.64 (t, J = 7.7 Hz, 4H, CH (Ar)), 7.73 (d, J = 7.4 Hz, 1H, CH (Ar)), 8.47 (d, J = 5.0 Hz, 4H, CH (Ar)). ^{13}C NMR (400 Hz, $CDCl_3$): δ_C 17.8, 18.8, 29.5, 31.3, 58.4, 59.2, 76.6, 76.9, 77.2, 122.1, 123.3, 127.4, 128.1, 128.6, 129.0, 129.8, 130.4, 135.7, 136.9, 138.8, 139.5, 140.4, 148.2, 158.5, 169.1, 172.9. HRMS (ES^+). Calcd for $C_{46}H_{50}N_7O_3$ [M + H]: m/z 720.3657. Found: m/z 720.3648. IR (KBr, cm^{-1}): 3445, 2960, 2924, 2852, 1638, 1570, 1474, 1434, 1384, 763.

10. HRMS (ES^+). Calcd for $C_{46}H_{49}N_7O_3Zn_2$ [M]: m/z 847.2145. Found: m/z 847.2155. IR (KBr, cm^{-1}): 3483, 2963, 1734, 1609, 1574, 1528, 1485, 1445, 1251, 1170, 1100, 1034, 866.

L11. ^1H NMR (400 MHz, $CDCl_3$): δ_H 1.49−2.40 (m, 4H, ring CH_2), 2.94−3.13 (m, 2H, ring CH_2), 3.64−4.06 (m, 12H, $PhCH_2N-$ and $-NCH_2Pyr$), 4.27−4.64 (m, 1H, $C_\alpha H$), 7.10−7.19 (m, 4H, CH (Ar)), 7.26−7.71 (m, 15H, CH (Ar)), 8.47−8.58 (m, 4H, CH (Ar)). ^{13}C NMR (400 Hz, $CDCl_3$): δ_C 24.6, 29.5, 29.8, 48.6, 58.4, 58.8, 59.1, 59.4, 76.8, 77.2, 77.4, 77.5, 122.4, 122.6, 123.8, 124.0, 127.4, 127.7, 129.5, 130.6, 136.2, 137.2, 137.4, 139.0, 140.0, 148.5, 148.8, 157.9, 158.7. HRMS (ES^+). Calcd for $C_{44}H_{44}N_7O_3$ [M + H]: m/z 706.3500. Found: m/z 706.3512. IR (KBr, cm^{-1}): 3435, 2924, 1621, 1595, 1438, 1384, 1299, 766.

11. HRMS (ES^+). Calcd for $C_{44}H_{43}N_7O_3Zn_2$ [M]: m/z 845.1988. Found: m/z 845.1991. IR (KBr, cm^{-1}): 3470, 2924, 1727, 1609, 1575, 1483, 1445, 1275, 1250, 1170, 1100, 1033, 981, 766.

L12. ^1H NMR (400 MHz, $CDCl_3$): δ_H 0.86 (dd, J = 10.0 and 6.6 Hz, 6H, $-CH(CH_3)_2$), 1.39−1.69 (m, 3H, $C_\beta H_2$ and $C_\gamma H$), 3.61−4.03 (m, 12H, $PhCH_2N-$ and $-NCH_2Pyr$), 4.44−4.53 (m, 1H, $C_\alpha H$), 6.10 (d, J = 8.4 Hz, 1H, NH), 7.13 (t, J = 6.2 Hz, 4H, CH (Ar)), 7.26−7.30 (m, 2H, CH (Ar)), 7.36−7.57 (m, 8H, CH (Ar)), 7.60−7.73 (m, 5H, CH (Ar)), 8.48 (d, J = 4.5 Hz, 4H, CH (Ar)), 10.68 (s_{br}, 1H, COOH). ^{13}C NMR (400 Hz, $CDCl_3$): δ_C 22.1, 22.6, 24.8, 29.5, 30.8, 41.8, 51.9, 58.4, 59.2, 76.6, 76.9, 77.2, 122.2, 123.4, 127.3, 128.3, 128.5, 129.2, 129.9, 130.4, 135.6, 136.9, 138.5, 139.6, 140.4, 148.3, 158.3, 168.8, 174.1. HRMS (ES^+). Calcd for $C_{45}H_{48}N_7O_3$ [M + H]: m/z 734.8313. Found: m/z 734.8324. IR (KBr, cm^{-1}): 3439, 2923, 1639, 1594, 1570, 1473, 1433, 1366, 1150, 762, 727.

12. HRMS (ES^+). Calcd for $C_{45}H_{47}N_7O_3Zn_2$ [M]: m/z 861.2301. Found: m/z 861.2322. IR (KBr, cm^{-1}): 3445, 2959, 2924, 1636, 1575, 1445, 1263, 1229, 1177, 1033, 765.

L13. ^1H NMR (400 MHz, $CDCl_3$): δ_H 1.20 (d, J = 7.1 Hz, 3H, $-CH_3$), 3.69 (s, 4H, $PhCH_2N-$), 3.83 (s, 8H, $-NCH_2Pyr$), 4.25−4.34 (m, 1H, $C_\alpha H$), 6.27 (d, J = 6.8 Hz, 1H, NH), 7.12 (t, J = 6.0 Hz, 4H, CH (Ar)), 7.25−7.31 (m, 2H, CH (Ar)), 7.35 (s, 2H, CH (Ar)), 7.38−7.48 (m, 2H, CH (Ar)), 7.52 (d, J = 7.8 Hz, 4H, CH (Ar)), 7.63 (t, J = 7.7 Hz, 4H, CH (Ar)), 7.77 (d, J = 7.3 Hz, 1H, CH (Ar)), 8.48 (d, J = 4.5 Hz, 4H, CH (Ar)), 9.24 (s_{br}, 1H, COOH). ^{13}C NMR (400 Hz, $CDCl_3$): δ_C 18.6, 29.8, 49.7, 58.8, 59.6, 76.8, 77.2, 77.5, 122.4, 123.6, 127.7, 128.5, 129.1, 129.5, 130.2, 130.5, 135.6, 137.1, 139.2, 140.0, 140.7, 148.6, 158.9, 168.5, 174.6. HRMS (ES^+). Calcd for $C_{42}H_{42}N_7O_3$ [M + H]: m/z 692.3344. Found: m/z 692.3351. IR (KBr, cm^{-1}): 3441, 2923, 2851, 1637, 1595, 1570, 1437, 1299, 1151, 765.

13. HRMS (ES^+). Calcd for $C_{42}H_{41}N_7O_3Zn_2$ [M]: m/z 819.1832. Found: m/z 819.1855. IR (KBr, cm^{-1}): 3506, 2925, 1731, 1609, 1574, 1531, 1485, 1446, 1251, 1170, 1100, 1033, 766.

L14. ^1H NMR (400 MHz, $CDCl_3$): δ_H 3.00−3.17 (m, 2H, $-CH_2Ph$), 3.63−3.92 (m, 12H, $PhCH_2N-$ and $-NCH_2Pyr$), 4.48−4.57 (m, 1H, $C_\alpha H$), 6.14 (d, J = 8.2 Hz, 1H, NH), 7.07−7.21 (m, 10H, CH (Ar)), 7.24−7.28 (m, 2H, CH (Ar)), 7.33−7.47 (m, 4H, CH (Ar)), 7.52 (d, J = 8.2 Hz, 4H, CH (Ar)), 7.56−7.67 (m, 5H, CH (Ar)), 8.46 (d, J = 5.0 Hz, 4H, CH (Ar)). ^{13}C NMR (400 Hz, $CDCl_3$): δ_C 37.9, 54.6, 58.7, 59.4, 76.8, 77.2, 77.4, 77.5, 122.4, 123.7, 126.7, 127.6, 128.3, 128.5, 129.4, 129.6, 130.1, 130.5, 135.8, 137.1, 137.2, 138.7, 139.9, 140.6, 148.3, 148.5, 158.6, 169.1, 173.2. HRMS (ES^+). Calcd for $C_{48}H_{46}N_7O_3$ [M + H]: m/z 768.3657. Found: m/z 768.3685. IR (KBr, cm^{-1}): 3424, 3060, 2922, 2849, 1644, 1593, 1569, 1433, 1223, 1150, 907, 762, 728, 700.

14. HRMS (ES^+). Calcd for $C_{48}H_{45}N_7O_3Zn_2$ [M]: m/z 895.2145. Found: m/z 895.2163. IR (KBr, cm^{-1}): 3453, 2917, 2849, 1735, 1636, 1575, 1540, 1487, 1262, 1229, 1176, 1033, 765.

dx.doi.org/10.1021/ic3008393 | Inorg. Chem. 2012, 51, 8284−8291

L15. ^{1}H NMR (400 MHz, $CDCl_3$): δ_H 3.68 (s, 4H, $PhCH_2N-$), 3.83 (s, 8H, $-NCH_2Pyr$), 4.59−4.67 (m, 1H, $C_\alpha H$), 6.30 (d, J = 7.5 Hz, 1H, NH), 6.58 (d, J = 8.3 Hz, 2H, CH (Ar)), 6.78 (d, J = 8.3 Hz, 2H, CH (Ar)), 7.15 (t, J = 6.8 Hz, 4H, CH (Ar)), 7.21−7.74 (m, 15H, CH (Ar)), 8.46 (d, J = 4.8 Hz, 4H, CH (Ar)), 9.99 (s, 1H, COOH). ^{13}C NMR (400 MHz, $CDCl_3$): δ_C 37.0, 54.7, 58.6, 59.0, 115.8, 122.7, 123.8, 127.3, 128.7, 128.8, 129.0, 130.2, 130.4, 130.6, 135.3, 137.6, 138.5, 139.7, 140.6, 148.2, 156.1, 158.1, 169.0, 173.8. HRMS (ES^+). Calcd for $C_{48}H_{46}N_7O_4$ [M + H]: m/z 784.3606. Found: m/z 784.3612. IR (KBr, cm^{-1}): 3439, 2923, 1633, 1516, 1446, 1261, 1177, 1034, 765.

15. HRMS (ES^+). Calcd for $C_{48}H_{45}N_7O_4Zn_2$ [M]: m/z 911.2094. Found: m/z 911.2082. IR (KBr, cm^{-1}): 3476, 2923, 1735, 1609, 1523, 1484, 1445, 1274, 1251, 1170, 1034, 767.

L16. ^{1}H NMR (400 MHz, $CDCl_3$): δ_H 3.65 (s, 4H, $-PhCH_2N$), 3.72 (s, 8H, $-NCH_2Pyr$), 7.05 (t, J = 5.6 Hz, 4H, CH (Ar)), 7.34−7.60 (m, 13H, CH (Ar)), 7.82 (d, J = 8.0 Hz, 1H, CH (Ar)), 8.45 (d, J = 4.8 Hz, 4H, CH (Ar)), 10.5 (s, 1H, COOH). ^{13}C NMR (400 MHz, $CDCl_3$): δ_C 59.2, 59.8, 122.1, 123.4, 127.0, 128.4, 128.4, 129.6, 130.0, 134.7, 136.7, 138.2, 140.5, 141.2, 148.5, 158.8, 170.8, 173.1. HRMS (ES^+). Calcd for $C_{39}H_{37}N_6O_2$ [M + H]: m/z 621.2973. Found: m/z 621.2982. IR (KBr, cm^{-1}): 3441, 3054, 2921, 2849, 1689, 1592, 1569, 1473, 1433, 1364, 1248, 1128, 1092, 1047, 762.

16. HRMS (ES^+). Calcd for $C_{39}H_{36}N_6O_2Zn_2$ [M]: m/z 748.1461. Found: m/z 748.1454. IR (KBr, cm^{-1}): 3475, 1741, 1605, 1574, 1445, 1251, 1176, 1101, 1034, 765.

■ ASSOCIATED CONTENT

Ⓢ Supporting Information

Full synthetic details, copies of ^{1}H and ^{13}C NMR spectra, and analytical rpHPLC traces. This material is available free of charge via the Internet at http://pubs.acs.org.

■ AUTHOR INFORMATION

Corresponding Author

*E-mail: Patrick.gunning@utoronto.ca. Tel.: 905-828-5354. Fax: 905-569-5425.

Notes

The authors declare no competing financial interest.

■ ACKNOWLEDGMENTS

This work was supported by NSERC (P.T.G.), University of Toronto (P.T.G.), the Leukemia and Lymphoma Society of Canada, and an NSERC Canada Graduate Scholarship (to J.A.D.).

■ REFERENCES

(1) Drewry, J. A.; Fletcher, S.; Yue, P.; Marushchak, D.; Zhao, W.; Sharmeen, S.; Zhang, X.; Schimmer, A. D.; Gradinaru, C.; Turkson, J.; Gunning, P. T. *Chem. Commun.* **2010**, *46*, 892−894.

(2) Fletcher, S.; Drewry, J. A.; Shahani, V. M.; Page, B. D. G.; Gunning, P. T. *Biochem. Cell Biol.* **2009**, *87*, 825−833.

(3) Anderson, D.; Koch, C. A.; Grey, L.; Ellis, C.; Moran, M. F.; Pawson, T. *Science (New York, N.Y.)* **1990**, *250*, 979−982.

(4) Moran, M. F.; Koch, C. A.; Anderson, D.; Ellis, C.; England, L.; Martin, G. S.; Pawson, T. *Proc. Natl. Acad. Sci. U.S.A.* **1990**, *87*, 8622−8626.

(5) Grebien, F.; Hantschel, O.; Wojcik, J.; Kaupe, I.; Kovacic, B.; Wyrzucki, A. M.; Gish, G. D.; Cerny-Reiterer, S.; Koide, A.; Beug, H.; Pawson, T.; Valent, P.; Koide, S.; Superti-Furga, G. *Cell* **2011**, *147*, 306−319.

(6) Li, L.; Tibiche, C.; Fu, C.; Kaneko, T.; Moran, M. F.; Schiller, M. R.; Li, S. S.; Wang, E. *Genome Res.* **2012**, 1−10.

(7) Bradshaw, J. M.; Grucza, R. A.; Ladbury, J. E.; Waksman, G. *Biochemistry* **1998**, *37*, 9083−9090.

(8) Bradshaw, J. M.; Waksman, G. *Adv. Protein Chem.* **2002**, *61*, 161−210.

(9) Grucza, R. A.; Bradshaw, J. M.; Fütterer, K.; Waksman, G. *Med. Res. Rev.* **1999**, *19*, 273−293.

(10) Siddiquee, K.; Zhang, S.; Guida, W. C.; Blaskovich, M. A.; Greedy, B.; Lawrence, H. R.; Yip, M. L.; Jove, R.; McLaughlin, M. M.; Lawrence, N. J.; Sebti, S. M.; Turkson, J. *Proc. Natl. Acad. Sci. U.S.A.* **2007**, *104*, 7391−7396−6.

(11) Levitzki, A.; Gazit, A. *Science (New York, N.Y.)* **1995**, *267*, 1782−1788.

(12) Gunning, P. T.; Glenn, M. P.; Siddiquee, K. A.; Katt, W. P.; Masson, E.; Sebti, S. M.; Turkson, J.; Hamilton, A. D. *ChemBioChem* **2008**, *9*, 2800−2803.

(13) *Science (New York, N.Y.)* **1995**, *267*, 1347−1349.

(14) *Science (New York, N.Y.)* **1994**, *264*, 1415−1421.

(15) Herbst, R. S.; Onn, A.; Mendelsohn, J. *Cancer Treat. Res.* **2003**, *115*, 19−72.

(16) Burger, S. K.; Lacasse, M.; Verstraelen, T.; Drewry, J.; Gunning, P.; Ayers, P. W. *J. Chem. Theory Comput.* **2012**, *8*, 554−562.

(17) Müller, J.; Schust, J.; Berg, T. *Anal. Biochem.* **2008**, *375*, 249−254.

(18) Mazouchi, A.; Liu, B.; Bahram, A.; Gradinaru, C. C. *Anal. Chim. Acta* **2011**, *688*, 61−69.

(19) Simpson, C. D.; Mawji, I. A.; Anyiwe, K.; Williams, M. A.; Wang, X.; Venugopal, A. L.; Gronda, M.; Hurren, R.; Cheng, S.; Serra, S.; Zavareh, R. B.; Datti, A.; Wrana, J. L.; Ezzat, S.; Schimmer, A. D. *Cancer Res.* **2009**, *69*, 2739−2747.